

Constant-sound-speed parametrization for Nambu–Jona-Lasinio models of quark matter in hybrid stars

Ignacio F. Ranea-Sandoval^{*}

Grupo de Gravitación, Astrofísica y Cosmología, Facultad de Ciencias; Astronómicas y Geofísicas, Universidad Nacional de La Plata, Paseo del Bosque S/N (1900), La Plata, Argentina and CONICET, Godoy Cruz 2290, 1425 Buenos Aires, Argentina

Sophia Han[†]

Department of Physics and Astronomy, University of Tennessee, Knoxville, Tennessee 37996, USA; Physics Division, Oak Ridge National Laboratory, Oak Ridge, Tennessee 37831, USA; and Physics Department, Washington University, St. Louis, Missouri 63130, USA

Milva G. Orsaria[‡]

Grupo de Gravitación, Astrofísica y Cosmología, Facultad de Ciencias; Astronómicas y Geofísicas, Universidad Nacional de La Plata, Paseo del Bosque S/N (1900), La Plata, Argentina and CONICET, Godoy Cruz 2290, 1425 Buenos Aires, Argentina

Gustavo A. Contrera[§]

IFLP, UNLP, CONICET, Facultad de Ciencias Exactas, calle 49 y 115, La Plata, Argentina and Grupo de Gravitación, Astrofísica y Cosmología, Facultad de Ciencias Astronómicas y Geofísicas, Universidad Nacional de La Plata, Paseo del Bosque S/N (1900), La Plata, Argentina

Fridolin Weber^{||}

Department of Physics, San Diego State University, 5500 Campanile Drive, San Diego, California 92182, USA and Center for Astrophysics and Space Sciences, University of California, San Diego, La Jolla, California 92093, USA

Mark G. Alford[¶]

Physics Department, Washington University, St. Louis, Missouri 63130, USA

(Received 8 January 2016; published 27 April 2016)

The discovery of pulsars as heavy as 2 solar masses has led astrophysicists to rethink the core compositions of neutron stars, ruling out many models for the nuclear equations of state (EoS). We explore the hybrid stars that occur when hadronic matter is treated in a relativistic mean-field approximation and quark matter is modeled by three-flavor local and nonlocal Nambu–Jona-Lasinio (NJL) models with repulsive vector interactions. The NJL models typically yield equations of state that feature a first-order transition to quark matter. Assuming that the quark-hadron surface tension is high enough to disfavor mixed phases and restricting to EoSs that allow stars to reach 2 solar masses, we find that the appearance of the quark-matter core either destabilizes the star immediately (this is typical for nonlocal NJL models) or leads to a very short hybrid star branch in the mass-radius relation (this is typical for local NJL models). Using the constant-sound-speed parametrization we can see that the reason for the near absence of hybrid stars is that the transition pressure is fairly high and the transition is strongly first order.

DOI: [10.1103/PhysRevC.93.045812](https://doi.org/10.1103/PhysRevC.93.045812)

I. INTRODUCTION

The composition and properties of neutron stars, which are among the densest objects in the universe, are not well understood theoretically. However, measurements of the masses and radii of these stars are putting strong constraints

on the equation of state (EoS), ruling out many theoretical models proposed over the years or at least restricting the allowed values of their free parameters. Especially the recent discovery of two neutron stars with masses $\sim 2M_{\odot}$, by means of the Shapiro delay for J1614 – 2230 [1] and white dwarf spectroscopy for J0348 + 0432 [2], imposes severe constraints on models for the EoS of superdense matter in the cores of neutron stars [3–7].

Inside cold neutron stars, the nuclear matter, which is subject to extreme conditions of high density but low temperature, could undergo a phase transition, melting hadrons into quarks. Theoretical calculations have suggested that the deconfinement transition of hadronic matter at low temperature but high density is of first order [8,9]. For neutron stars,

^{*}iranea@fcaglp.unlp.edu.ar

[†]jhan@physics.wustl.edu

[‡]morsaria@fcaglp.unlp.edu.ar

[§]contrera@fisica.unlp.edu.ar

^{||}fweber@mail.sdsu.edu

[¶]alford@wuphys.wustl.edu

this can be modeled with a hybrid EoS, which describes neutron-star matter at low densities in terms of hadrons and of deconfined quarks at high densities, assuming a sharp first-order phase transition between hadronic and quark matter and considering a generic parametrization of the quark matter EoS with a density-independent speed of sound, known as the “constant-sound-speed” (CSS) parametrization [10,11]. We use the CSS parametrization to gain insight into the range of possible hybrid stars that is predicted by local and nonlocal Nambu–Jona-Lasinio (NJL) models of quark matter combined with a relativistic mean-field model of nuclear matter.

Previous analyses of hybrid stars using NJL models of the quark-matter EoS have employed various types of the NJL model, including models with vector interactions and diquark channels to allow for color superconductivity [3,12,13], models with eight quark interactions [14,15], and nonlocal NJL models [4,16–18]. Quark matter has also been treated by other methods, such as perturbative QCD extrapolated down to the densities of interest [19], bag models [20–23], the field correlator method [24], and Dyson-Schwinger equations [25].

In this paper we describe quark matter by the widely studied NJL model [26–29] with both local and nonlocal interactions. The nonlocal NJL model includes a form factor in the quark-quark interactions that can be used to simulate the effects of confinement (by generating a quark propagator without poles at real energies [30–33]) and also functions as a natural regulator. In fact, nonlocality arises naturally in the context of several successful approaches to low-energy quark dynamics as, for example, one gluon exchange [34–36] (as in this work), the instanton liquid model [37,38], and the Dyson-Schwinger resummation techniques [39,40]. Lattice QCD calculations [41] also indicate that quark interactions should act over a certain range in momentum space. Moreover, several studies [33,42–45] have shown that nonlocal chiral quark models provide a satisfactory description of hadron properties at zero temperature and density. In our NJL calculations we also include vector interactions and the formation of a chiral condensate, but not diquark condensation (color superconductivity [46]).

The main questions that are being addressed in this paper are as follows. Does the range of physically plausible parameters of the NJL quark matter EoS allow for hybrid stars, and, if so, how long is the hybrid star branch, and are there observable signatures such as a disconnected third-family branch of hybrid stars as noted in Refs. [15,47,48]? Does the CSS parametrization adequately capture the functional form of the NJL quark-matter EoS? Can the CSS parametrization be used to understand the mass-radius characteristics of NJL hybrid stars?

In particular, previous analysis of hybrid stars using the CSS parametrization of possible quark-matter EoSs has shown that it is easiest to achieve masses of $2M_\odot$ and above if the quark matter is stiff, with a high speed of sound $c_{\text{QM}}^2 \gtrsim 0.4$ [24]. If the hadron-quark transition is at low pressure, then a long hybrid branch can exist in the mass-radius plane; if the transition is at high pressure then the hybrid branch, if it exists, tends to be very small. In this paper we see that the

NJL models studied here are of the “high-transition-pressure” type.

The paper is organized as follows. In Sec. II we describe briefly the models for the hadron and quark phases of the hybrid stars. In Sec. III we review the CSS parametrization proposed in Ref. [11] and check to what degree it can accurately characterize our NJL EoSs. In Sec. IV we discuss the hybrid stars resulting from our NJL models, and in Sec. V we give our conclusions.

II. DENSE MATTER IN THE CORES OF HYBRID STARS

A. The outer core

We model the matter in the outer core of a hybrid star using a nonlinear relativistic mean-field theory [49–53], where baryons (neutrons, protons, hyperons, and Δ states) interact via the exchange of scalar, vector, and isovector mesons (σ , ω , and ρ mesons, respectively). Replacing all baryon currents in the field equations with their respective ground-state expectation values, we arrive at a system of mean-field equations at zero temperature given by

$$\begin{aligned} m_\sigma^2 \sigma &= -\frac{dU}{d\sigma} + \sum_B \frac{2J_B + 1}{2\pi^2} g_{\sigma B} \\ &\quad \times \int_0^{k_B} p^2 dp \frac{m_B - g_{\sigma B} \sigma}{[p^2 + (m_B - g_{\sigma B} \sigma)^2]^{1/2}}, \\ m_\omega^2 \omega_0 &= \sum_B g_{\omega B} n_B, \\ m_\rho^2 \rho_{03} &= \sum_B g_{\rho B} I_{3B} n_B, \end{aligned} \quad (1)$$

where I_{3B} and J_B are the three components of isospin and spin, respectively, and k_B is the Fermi momentum of a baryon of type B . The baryon-meson coupling constants $g_{\sigma B} = x_{\sigma B} g_\sigma$, $g_{\omega B} = x_{\omega B} g_\omega$, and $g_{\rho B} = x_{\rho B} g_\rho$ are expressed in terms of the scalar, vector, and isovector coupling constants g_σ , g_ω , and g_ρ of the hadronic model parametrizations (GM1 and NL3) studied in this paper [4,54,55]. Following Ref. [56] we take $x_{\sigma B} = 0.7$ and $x_{\omega B} = x_{\rho B} = 1$. The quantity U in Eq. (1) denotes the nonlinear σ -meson potential, representing the self-interactions of the scalar σ field. It can be written as

$$U = [b_1 m_N + b_2 (g_\sigma \sigma)] (g_\sigma \sigma)^3, \quad (2)$$

with $b_{1,2}$ denoting constants determined by the properties of hadronic matter. The quantity m_N is the nucleon mass. Solving Eq. (1) together with the charge neutrality condition and baryonic number conservation, we obtain the total pressure and the energy density of the hadronic matter in the outer core of the hybrid star (for details, see Refs. [56,57]).

B. The inner core

To describe the matter in the inner core of the hybrid star we use a local and nonlocal extension of the NJL model. The nonlocal NJL extension includes nonlocal interactions and has several advantages over the local NJL model (for details, see Ref. [4] and references therein).

1. The nonlocal NJL model

For this model, the mean-field thermodynamic potential at zero temperature is given by [4]

$$\begin{aligned}
 \Omega^{\text{NL}}(M_f, 0, \mu_f) &= -\frac{N_c}{\pi^3} \sum_{f=u,d,s} \int_0^\infty dp_0 \int_0^\infty dp p^2 \\
 &\times \ln \left\{ [\widehat{\omega}_f^2 + M_f^2(\omega_f^2)] \frac{1}{\omega_f^2 + m_f^2} \right\} \\
 &- \frac{N_c}{\pi^2} \sum_{f=u,d,s} \int_0^{\sqrt{\mu_f^2 - m_f^2}} dp p^2 [(\mu_f - E_f)\theta(\mu_f - m_f)] \\
 &- \frac{1}{2} \left[\sum_{f=u,d,s} \left(\bar{\sigma}_f \bar{S}_f + \frac{G_S}{2} \bar{S}_f^2 \right) + \frac{H}{2} \bar{S}_u \bar{S}_d \bar{S}_s \right] \\
 &- \sum_{f=u,d,s} \frac{\varpi_f^2}{4G_V}, \quad (3)
 \end{aligned}$$

where $N_c = 3$ (as we are considering three quark colors), $E_f = \sqrt{p^2 + m_f^2}$, and $\omega_f^2 = (p_0 + i\mu_f)^2 + p^2$. The constituent quark masses, M_f , are treated as momentum-dependent quantities and are given by

$$M_f(\omega_f^2) = m_f + \bar{\sigma}_f g(\omega_f^2), \quad (4)$$

where $g(\omega_f^2)$ denotes a form factor which we take to be Gaussian, $g(\omega_f^2) = \exp(-\omega_f^2/\Lambda^2)$.

The inclusion of vector interactions shifts the quark chemical potential by

$$\mu_f \rightarrow \widehat{\mu}_f = \mu_f - g(\omega_f^2)\varpi_f, \quad (5)$$

where ϖ_f represents the vector mean fields related to the vector current interaction. The inclusion of the form factor in Eq. (5) is a particular feature of the nonlocal model, which renders the shifted chemical potential momentum dependent. The squared four momenta, ω_f^2 , in the dressed part of the thermodynamic potential are modified as

$$\omega_f^2 \rightarrow \widehat{\omega}_f^2 = (p_0 + i\widehat{\mu}_f)^2 + p^2. \quad (6)$$

Note that to avoid a recursive problem, as discussed in Refs. [16,58,59], the quark chemical potential shift does not affect the nonlocal form factor $g(\omega_f^2)$. In this work we use the parameters listed in Table I for the nonlocal NJL model.

TABLE I. Sets of parameters used for the nonlocal NJL model calculations presented in this paper.

Parameters	Set I	Set II	Set III
\bar{m} (MeV)	5.0	5.5	6.2
m_s (MeV)	119.3	127.8	140.7
Λ (MeV)	843.0	780.6	706.0
$G_S \Lambda^2$	13.34	14.48	15.04
$H \Lambda^5$	-273.75	-267.24	-337.71

As was proven in Ref. [60], within the stationary phase approximation, the mean-field values of the auxiliary fields, \bar{S}_f , are related to the mean-field values of the scalar fields $\bar{\sigma}_f$. They are given by

$$\bar{S}_f = -16N_c \int_0^\infty dp_0 \int_0^\infty dp \frac{p^2}{(2\pi)^3} g(\omega_f^2) \frac{M_f(\omega_f^2)}{\widehat{\omega}_f^2 + M_f^2(\omega_f^2)}. \quad (7)$$

The mean-field values of $\bar{\sigma}_f$ and ϖ_f are obtained via minimizing the thermodynamic potential with respect to variations in these quantities; that is,

$$\frac{\partial \Omega^{\text{NL}}}{\partial \bar{\sigma}_f} = 0, \quad \frac{\partial \Omega^{\text{NL}}}{\partial \varpi_f} = 0. \quad (8)$$

The relevant mean-field flavor fields are $\bar{\sigma}_u$, $\bar{\sigma}_d$, and $\bar{\sigma}_s$.

2. The local NJL model

For the local SU(3) NJL model, we use the scheme and parameters of Refs. [4,61] (and references therein). At the mean-field level, the thermodynamic potential at zero temperature reads

$$\begin{aligned}
 \Omega^L(M_f, \mu) &= G_S \sum_{f=u,d,s} \langle \bar{\psi}_f \psi_f \rangle^2 + 4H \langle \bar{\psi}_u \psi_u \rangle \langle \bar{\psi}_d \psi_d \rangle \langle \bar{\psi}_s \psi_s \rangle \\
 &- 2N_c \sum_{f=u,d,s} \int_\Lambda \frac{d^3 p}{(2\pi)^3} E_f \\
 &- \frac{N_c}{3\pi^2} \sum_{f=u,d,s} \int_0^{p_{F_f}} dp \frac{p^4}{E_f} - G_V \sum_f \rho_f^2, \quad (9)
 \end{aligned}$$

where $N_c = 3$, $E_f = \sqrt{p^2 + M_f^2}$, and $p_{F_f} = \sqrt{\mu_f^2 - M_f^2}$. The constituent quark masses M_f are given by

$$M_f = m_f - 2G_S \langle \bar{\psi}_f \psi_f \rangle - 2H \langle \bar{\psi}_j \psi_j \rangle \langle \bar{\psi}_k \psi_k \rangle, \quad (10)$$

with $f, j, k = u, d, s$ indicating cyclic permutations. The vector interaction shifts the quark chemical potential according to

$$\mu_f \rightarrow \mu_f - 2G_V \rho_f, \quad (11)$$

where ρ_f is the quark number density of the quark field of flavor f in the mean-field approximation; that is,

$$\rho_f = \frac{N_c}{3\pi} [(\mu_f - 2G_V \rho_f)^2 - M_f^2]^{3/2}. \quad (12)$$

The mean-field values are determined from the solution of the gap equations, obtained by minimizing the thermodynamic potential with respect to the quark condensates $\langle \bar{\psi}_f \psi_f \rangle$,

$$\frac{\partial \Omega^L}{\partial \langle \bar{\psi}_f \psi_f \rangle} = 0, \quad f = u, d, s. \quad (13)$$

C. The hadron-quark phase transition

Several theoretical works [15,19–21,48,62–64] have suggested that there might be a first-order phase transition between hadronic and quark matter at low temperatures. The density at which such a phase transition occurs is not known, but it is expected to occur at several times nuclear saturation density.

TABLE II. Sets of parameters used for the local NJL model calculations presented in this paper.

Parameters	Set IV	Set V
\bar{m} (MeV)	5.5	5.5
m_s (MeV)	135.7	140.7
Λ (MeV)	631.4	602.3
$G_s \Lambda^2$	3.67	3.67
$H \Lambda^5$	-9.29	-12.3

In a neutron star, such a transition can lead to two possible structures, depending on the surface tension between hadronic and quark matter [65–70].

If the surface tension between hadronic and quark matter is bigger than a critical value, which is estimated to be between around 5 to 40 MeV/fm² [65,67], then there is a sharp interface (Maxwell construction) between neutral hadronic matter and neutral quark matter. If the surface tension is below the critical value, then there is a mixed phase (Gibbs construction), with charge-separated domains of quark and hadronic matter occurring over a finite range of pressures. In this work we assume that the surface tension of the interface is high enough to ensure that the transition occurs at a sharp interface. This is a possible scenario, given the uncertainties in the value of the surface tension [65,68,71]. For a discussion of generic equations of state that continuously interpolate between the phases to model mixing or percolation, see Refs. [7,72,73].

III. THE CSS PARAMETRIZATION

The CSS parametrization assumes that there is a sharp interface between nuclear matter and quark matter and that the speed of sound in quark matter is pressure independent for pressures ranging from the first-order transition pressure up

to the maximum central pressure of a neutron star. The main features of the quark-matter EoS can then be captured by three parameters (see Fig. 1): the pressure p_{trans} at the transition, the discontinuity in energy density $\Delta\varepsilon$ at the transition, and the speed of sound c_{QM} in the high-density phase. For a given nuclear-matter EoS $\varepsilon_{\text{NM}}(p)$, the CSS parametrization of the EoS takes the form

$$\varepsilon(p) = \begin{cases} \varepsilon_{\text{NM}}(p), & p < p_{\text{trans}}, \\ \varepsilon_{\text{NM}}(p_{\text{trans}}) + \Delta\varepsilon + c_{\text{QM}}^{-2}(p - p_{\text{trans}}), & p > p_{\text{trans}}. \end{cases} \quad (14)$$

The values of the CSS parameters ($p_{\text{trans}}/\varepsilon_{\text{trans}}$, $\Delta\varepsilon/\varepsilon_{\text{trans}}$, c_{QM}^2) for the EoSs described in Sec. II are given in Tables III (non-local NJL) and IV (local NJL).

The discontinuity in the energy density $\Delta\varepsilon$ is a measure of how strongly the first-order phase transition is and determines the presence or absence of a connected hybrid star branch. When the central pressure rises just above p_{trans} one would expect a very small core of quark matter to appear. However, it can be shown [74–76] that, *independent* of the speed of sound in quark matter,

$$\begin{aligned} \Delta\varepsilon > \Delta\varepsilon_{\text{crit}} &\Rightarrow \text{no connected branch,} \\ \Delta\varepsilon < \Delta\varepsilon_{\text{crit}} &\Rightarrow \text{connected branch,} \end{aligned} \quad (15)$$

where $\frac{\Delta\varepsilon_{\text{crit}}}{\varepsilon_{\text{trans}}} = \frac{1}{2} + \frac{3}{2} \frac{p_{\text{trans}}}{\varepsilon_{\text{trans}}}$.

In other words, if the energy density jump at the transition is bigger than $\Delta\varepsilon_{\text{crit}}$, then the quark-matter core, no matter how small, destabilizes the star, and the mass-radius relationship contains no branch of hybrid stars connected to the hadronic branch. It must be emphasized strongly that this conclusion is independent of the speed of sound in quark matter and that the criterion (15) is valid independent of how pressure-

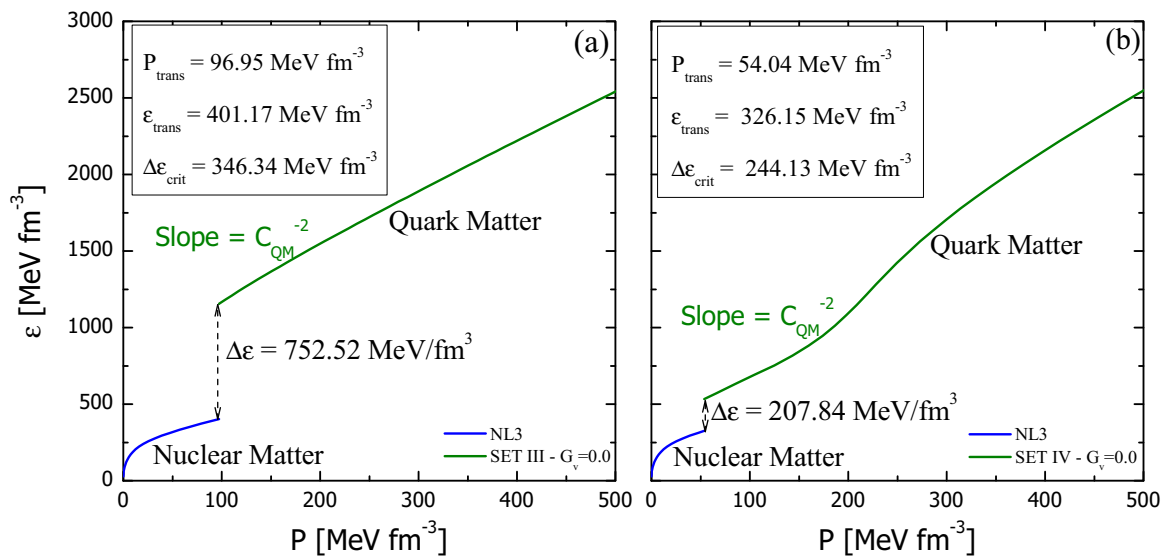


FIG. 1. EoS, $\varepsilon(p)$, for dense matter without vector interaction, showing the energy density discontinuity $\Delta\varepsilon$ between hadronic matter (NL3) and quark matter. For quark matter modeled by nonlocal NJL SET III (a), the discontinuity is greater than $\Delta\varepsilon_{\text{crit}}$ (15), so there is no stable connected hybrid branch. In contrast, the local NJL SET IV (b) has a smaller discontinuity $\Delta\varepsilon < \Delta\varepsilon_{\text{crit}}$, which leads to a connected but very short hybrid branch (see Table IV).

TABLE III. Properties of the compact stars arising from quark matter obeying the nonlocal NJL EoS. We show results for two hadronic EoSs, GM1 and NL3, and for various NJL parameter values (sets I, II, III; see Table I) and vector couplings G_V . For each case we show the three CSS parameters that characterize the quark-matter EoS (see Sec. III), along with the mass and radius of the heaviest star, and the mass range ΔM of the hybrid branch, obtained from the CSS parameters and from the original nonlocal NJL EoS.

EoS	G_V/G_S	$p_{\text{trans}}/\epsilon_{\text{trans}}$	$\Delta\epsilon/\epsilon_{\text{trans}}$	c_{QM}^2	$M_{\text{max}} (M_{\odot})$	R_M (km)	$\Delta M (M_{\odot})$ (CSS)	$\Delta M (M_{\odot})$ (NJL)		
GM1	Set I	0.00					No phase transition			
		0.05	0.25	0.78	0.13	2.10	13.36	5.1×10^{-6}	$<10^{-5}$	
		0.09	0.27	0.83	0.26	2.17	13.19	1.4×10^{-6}	$<10^{-5}$	
	Set II	0.00	0.24	1.21	0.22	2.08	13.39	0	0	
		0.05	0.28	1.09	0.27	2.18	13.18	0	0	
		0.09	0.31	0.96	0.29	2.25	12.97	$<10^{-6}$	$<10^{-5}$	
	Set III	0.00	0.24	1.35	0.26	2.09	13.38	0	0	
		0.05	0.29	1.12	0.32	2.21	13.10	0	0	
		0.09	0.33	0.87	0.46	2.29	12.78	1.1×10^{-6}	$<10^{-5}$	
	NL3	Set I	0.00					No phase transition		
			0.05						No phase transition	
			0.09						No phase transition	
Set II		0.00						No phase transition		
		0.05	0.27	1.46	0.17	2.37	14.59	0	0	
		0.09	0.29	1.39	0.25	2.46	14.49	0	0	
Set III		0.00	0.24	1.87	0.23	2.27	14.66	0	0	
		0.05	0.28	1.65	0.29	2.42	14.54	0	0	
		0.09	0.32	1.42	0.36	2.54	14.40	0	0	

independent the speed of sound in quark matter is. It is only for predictions of the presence or absence of *disconnected* branches or for properties of stable hybrid stars (mass, radius) that the CSS parametrization relies on the assumption of a pressure-independent speed of sound.

In Figs. 2 and 3 we plot c_{QM}^2 as a function of the pressure for all the quark-matter EoSs considered in Sec. II. We also show where the hadron-to-quark phase transitions occur, as dots (for the NL3 hadronic EoS) and triangles (for the GM1

hadronic EoS). NL3 is a stiffer EoS, and it undergoes the phase transition at lower p_{trans} .

In the local NJL models (Fig. 3) the speed of sound is only mildly sensitive to the NJL model parameters such as m_s (which increases from Set IV to Set V) and the vector coupling constant G_V . Moreover, above the hadron-to-quark phase transition the speed of sound shows only a moderate dependence on pressure, tending to stay within the range $c_{\text{QM}}^2 \sim 0.2$ to 0.3 . We therefore expect that the local NJL

TABLE IV. Properties of the compact stars arising from quark matter obeying the local NJL EoS. We show results for two hadronic EoSs, GM1 and NL3, and for various NJL parameter values (sets IV, V; see Table II) and vector couplings G_V . For each case we show the three CSS parameters that characterize the quark-matter EoS (see Sec. III), along with the mass and radius of the heaviest star and the mass range ΔM of the hybrid branch, obtained from the CSS parameters and from the original local NJL EoS.

EoS	G_V/G_S	$p_{\text{trans}}/\epsilon_{\text{trans}}$	$\Delta\epsilon/\epsilon_{\text{trans}}$	c_{QM}^2	$M_{\text{max}} (M_{\odot})$	R_M (km)	$\Delta M (M_{\odot})$ (CSS)	$\Delta M (M_{\odot})$ (NJL)
GM1	Set IV	0.00	0.20	0.39	0.33	1.93	5×10^{-2}	1.1×10^{-2}
		0.15	0.27	0.48	0.20	2.16	3×10^{-3}	1.4×10^{-3}
		0.30	0.32	0.66	0.23	2.27	2.5×10^{-4}	2.2×10^{-4}
	Set V	0.00	0.25	0.60	0.22	2.10	7.6×10^{-4}	4.9×10^{-4}
		0.15	0.30	0.85	0.19	2.23	1.7×10^{-6}	$<10^{-5}$
		0.30	0.34	0.84	0.27	2.30	1.9×10^{-6}	$<10^{-5}$
NL3	Set IV	0.00	0.17	0.64	0.31	1.84	2.8×10^{-4}	5.3×10^{-4}
		0.15	0.22	0.57	0.35	2.15	1.8×10^{-3}	2.6×10^{-3}
		0.30	0.27	0.59	0.24	2.39	8.4×10^{-4}	1.1×10^{-3}
	Set V	0.00	0.22	0.84	0.33	2.15	0	0
		0.15	0.27	0.84	0.21	2.39	2.8×10^{-6}	$<10^{-5}$
		0.30	0.31	0.99	0.21	2.52	0	0

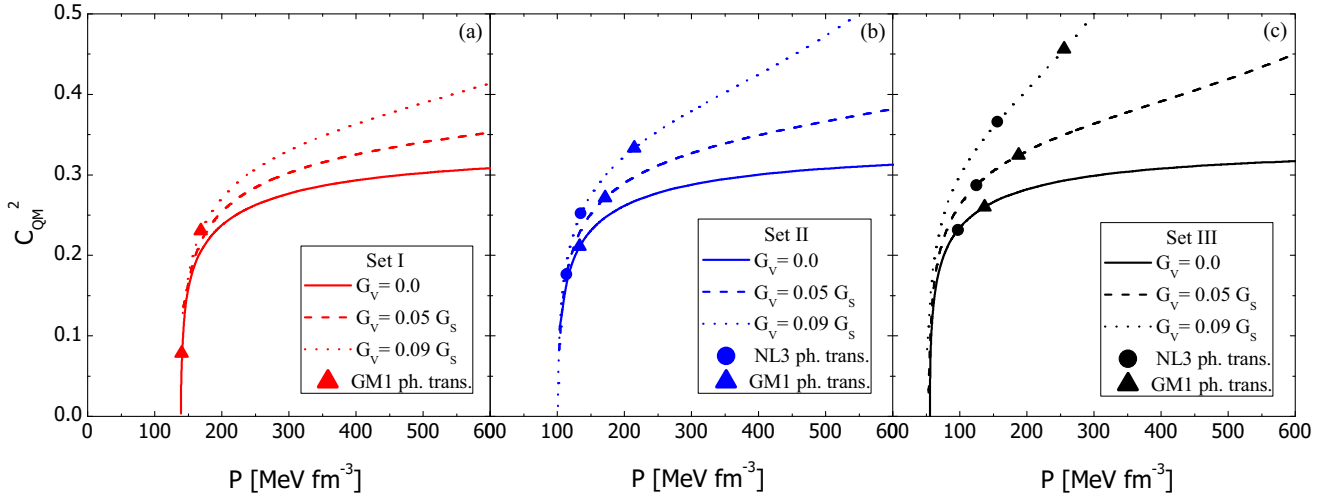


FIG. 2. Squared speed of sound for the nonlocal NJL quark matter model as a function of pressure. NL3 to quark-matter transitions are marked by dots; GM1 \rightarrow quark matter is marked by triangles. Solid lines show the behavior without vector interactions, while dashed and dotted lines represent the results for a finite vector interaction coupling constant. Left, middle, and right panels correspond to the nonlocal NJL model with parameter set I, panel (a); set II, panel (b); and set III, panel (c).

models will be reasonably accurately characterized by the CSS parametrization.

The nonlocal NJL model (Fig. 2), in contrast, shows great sensitivity to the NJL model parameters. As m_s and G_V increase we see that c_{QM}^2 varies more strongly with pressure. For higher values of m_s and G_V the nonlocal NJL model EoSs are outside the family of EoSs that can be accurately characterized by the CSS parametrization. However, as noted above, the criterion (15) for the presence of connected hybrid branches is independent of the speed of sound; the density dependence of c_{QM}^2 will only affect the CSS prediction of the presence of disconnected hybrid star branches.

IV. MASS-RADIUS RELATIONS

The CSS parametrization allows us to conveniently survey the mass-radius relationships for a large class of possible quark-matter equations of state. We first discuss how the form of the mass-radius relationship is determined by the CSS parameters; then we see where in the CSS parameter space the NJL quark matters EoSs are to be found.

The general dependence of the mass-radius relationship on the CSS parameters is shown schematically in Fig. 4. We have fixed c_{QM}^2 and we vary $p_{\text{trans}}/\varepsilon_{\text{trans}}$ and $\Delta\varepsilon/\varepsilon_{\text{trans}}$. There are four regions in the space of possible quark-matter EoSs

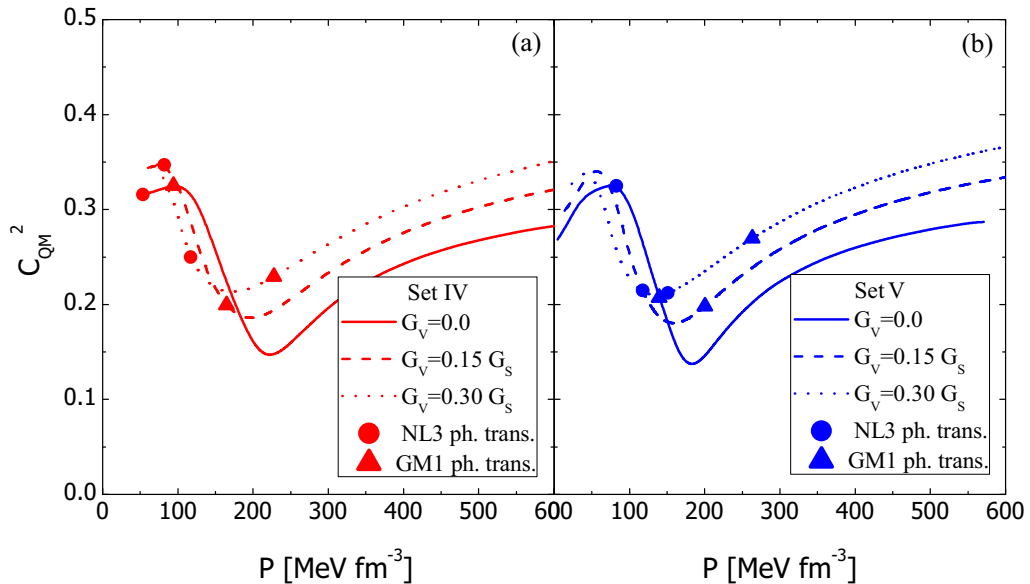


FIG. 3. Squared speed of sound for the local NJL quark-matter model as function of pressure. The symbols and line styles are similar to those in Fig. 2. Left and right panels correspond to the local NJL model with parameter set IV, panel (a); and set V, panel (b). Note that the local NJL model shows a more density-independent speed of sound and thus is more accurately characterized by the CSS parametrization than in the nonlocal case.

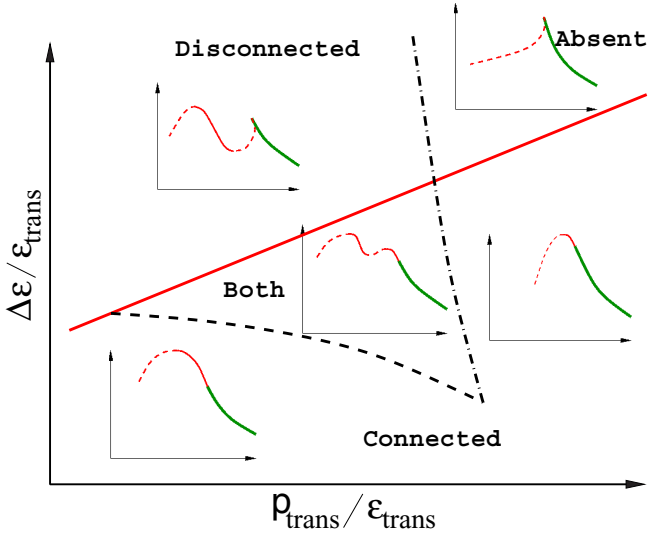


FIG. 4. Schematic phase diagram of the possible topologies of the mass-radius curve for compact stars: The hybrid branch may be connected to the nuclear branch (C) or disconnected (D), or both connected and disconnected branches may be present (B) or neither (A) [11]. The mass-radius curve in each region is depicted in inset graphs, in which the thick green line is the hadronic branch, the thin solid red lines the stable hybrid stars, and the thin dashed red lines the unstable hybrid stars. The thick straight (red) line in Fig. 4 is the critical line given by Eq. (15), above which there is no connected hybrid branch. We emphasize that this critical line is independent of the speed of sound in the quark matter and depends only on $\Delta\varepsilon/\varepsilon_{\text{trans}}$ and $\varepsilon_{\text{trans}}/p_{\text{trans}}$.

corresponding to four topologies of the mass-radius curve for compact stars: The hybrid branch may be connected to the nuclear branch (C) or disconnected (D), or both connected and disconnected branches may be present (B) or neither (A) [11]. The mass-radius curve in each region is depicted in inset graphs, in which the thick green line is the hadronic branch, the thin solid red lines the stable hybrid stars, and the thin dashed red lines the unstable hybrid stars. The thick straight (red) line in Fig. 4 is the critical line given by Eq. (15), above which there is no connected hybrid branch. We emphasize that this critical line is independent of the speed of sound in the quark matter and depends only on $\Delta\varepsilon/\varepsilon_{\text{trans}}$ and $\varepsilon_{\text{trans}}/p_{\text{trans}}$.

We see in Tables III and IV that each NJL model of the quark-matter EoS corresponds to a set of CSS parameters, i.e., to a value of c_{QM}^2 and a point in the accompanying $(p_{\text{trans}}/\varepsilon_{\text{trans}}, \Delta\varepsilon/\varepsilon_{\text{trans}})$ plane. In Figs. 5 and 6, we use black symbols to plot the CSS parameter values corresponding to the NJL models listed in Tables III and IV. In Fig. 5 the NJL models for quark matter are combined with nuclear matter described by the GM1 EoS. In Fig. 6 the nuclear matter is described by the NL3 EoS. To capture the variation in c_{QM}^2 , each figure has four panels, each one devoted to a small range of values of c_{QM}^2 . For example, in panel (a) of Fig. 5 we show the NJL models that have $c_{\text{QM}}^2 \approx 0.2$. One of them (the triangle point corresponding to GM1 + Set II) is in the ‘‘A’’ region, meaning that it gives no hybrid stars because its phase transition is so strongly first order. The others are all in the ‘‘C’’ region, meaning that their mass-radius relation includes a connected branch of hybrid stars. However, the connected branch is short, covering a range of no more than $0.05M_{\odot}$. (For other nuclear and quark models the hybrid branches are even shorter, covering a range of order of $10^{-3}M_{\odot}$ or less.)

It would be difficult to detect such a short hybrid branch in mass-radius observations.

In each panel in Figs. 5 and 6 there is a gray shaded region covering the equations of state that are ruled out because they give a maximum compact star mass below $2M_{\odot}$. The paler shading is for the lowest value of c_{QM}^2 that is associated with the panel, and the darker shading is for the highest value of c_{QM}^2 .

The ‘‘D’’ region (where disconnected hybrid star branches exist) and the ‘‘B’’ region (where both connected and disconnected hybrid star branches exist) are inside the gray shaded region, meaning that for the GM1 nuclear-matter EoS and for quark matter with $c_{\text{QM}}^2 \approx 0.2$ all CSS-compatible quark-matter EoSs that would give disconnected hybrid branches are ruled out because their heaviest star is too light.

The remaining panels of Fig. 6 show similar plots for the NJL EoSs with higher sound-speed values: $c_{\text{QM}}^2 \approx 0.25, 0.3$, and finally one for the GM1 + Set III EoS which has $c_{\text{QM}}^2 = 0.46$. We see that as c_{QM}^2 grows the B + D region (where disconnected hybrid branches exist) also grows, but always remains within the gray region, excluded by the $M_{\text{max}} > 2M_{\odot}$ constraint.

Most of the nonlocal NJL EoSs lack hybrid branches because the energy density jump at the transition is so large that the quark matter core immediately destabilizes the star. Even for the quark EoSs that are in the C region below the red line, the hybrid branch is very short. This is because those EoSs have high transition pressure ($p_{\text{trans}}/\varepsilon_{\text{trans}} \gtrsim 0.2$) so any star with central pressure high enough to develop a quark-matter core is already close to the central pressure at which the hadronic star would become unstable even without a quark-matter core, so when the core appears it easily ‘‘pushes the star over the edge’’ into instability.

To evaluate the sensitivity of our results to other parameters in the NJL model, we looked at two alternate parameter sets to see if they yielded longer hybrid branches.

First, to probe the effects of flavor mixing, we set the ’tHooft coupling constant H in the IV parametrization to zero. This corresponds to a local NJL model without flavor mixing. To reproduce the vacuum constituent quark masses, we set $G_S \Lambda^2 = 4.638$ and $m_s = 112.0$ MeV [29]. Because increasing G_V tends to result in smaller quark cores, we set $G_V = 0$. Even so, we found that setting H to zero further disfavors hybrid branches. For GM1 hadronic matter the resultant connected hybrid branches were even shorter ($\Delta M \sim 4 \times 10^{-4}M_{\odot}$) than in the case with $H \neq 0$. For NL3 hadronic matter there was no stable hybrid branch, where there had been a very short one when $H \neq 0$. We conclude that the ’tHooft flavor mixing term favors the appearance of a hybrid stable branch.

Second, to analyze how sensitive the results are to changes in the strange quark mass, we considered another parametrization for the local NJL model without vector coupling [77], with $\Lambda = 750$ MeV, $G_S^2 = 3.67$, $H\Lambda^5 = -8.54$, $m_u = m_d = 3.6$ MeV, and $m_s = 87$ MeV. With both GM1 and NL3 nuclear matter we found no hybrid branch. This could be attributed to the combination of two contributions: the lower strange quark mass increases the fraction of strange quarks at lower densities [29] and a weaker flavor mixing favors a faster increasing of strangeness fraction with rising density.

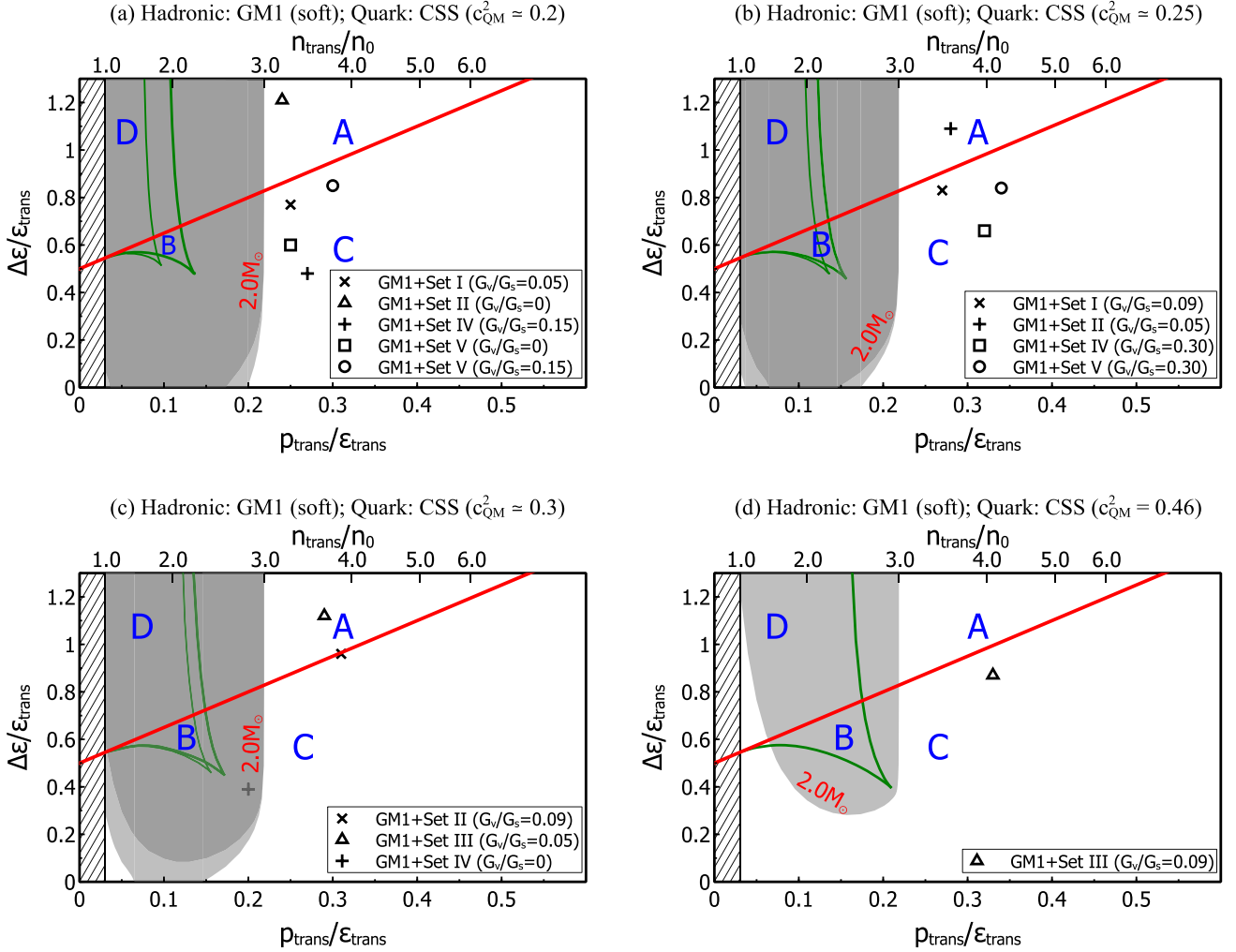


FIG. 5. Diagram showing (black symbols) where different quark matter parametrizations, for the local and nonlocal models, combined with GM1 nuclear matter, fall in the CSS parameter space. Panels (a), (b), (c), and (d) are for $c_{\text{QM}}^2 \simeq 0.2$, $c_{\text{QM}}^2 \simeq 0.25$, $c_{\text{QM}}^2 \simeq 0.3$, and $c_{\text{QM}}^2 = 0.46$, respectively. EoSs below the straight solid (red) line (regions B and C) yield a connected hybrid branch. EoSs within the shaded gray area are excluded because their heaviest star is below $2 M_{\odot}$. The hatched area at densities $n_{\text{trans}} < n_0$ is excluded because uniform nuclear matter is not stable in that region. See Tables III and IV.

The combination of these two contributions softens the quark-matter EoS and helps to destabilize hybrid stars. However, a color superconducting phase in the core could help to stabilize the star [63].

V. CONCLUSIONS

We have studied the hybrid stars that arise from quark matter modeled by local and nonlocal NJL models with vector interaction among the quarks. The reason for studying the nonlocal NJL model is that it is constructed to have the closest correspondence to QCD [33–44] and has a natural cutoff in the form of the momentum dependence of the effective quark masses. For the equation of state of hadronic matter we used the nonlinear relativistic mean-field model with two different parametrizations, GM1 (softer) and NL3 (stiffer). We assumed that the surface tension at the interface is high enough so that there is a sharp interface between the phases with no mixed phase.

The main physical conclusion is that the nonlocal NJL models that we studied typically give no hybrid stars, while the local NJL models sometimes give hybrid stars, but they cover a very small range of masses and radii (this is different from the behavior seen when the phase boundary is a mixed phase (Gibbs construction) [4,61]). According to Tables III and IV, the mass range is of order $10^{-3} M_{\odot}$ or less. One would expect a very small fraction of observed neutron stars to be in the hybrid branch, and they would be difficult to identify via mass and radius measurements, but it is possible that those stars, which would have very small quark-matter cores, might nonetheless have distinctive observable properties. One possibility is fast cooling if the quark-matter core had a high neutrino emissivity. Another is that the density discontinuity associated with the quark core might affect the frequency spectrum of nonradial oscillation modes [78], leading to signatures in the gravitational wave emission.

We found that in the NJL models that we studied the EoSs for quark matter are adequately represented by the CSS

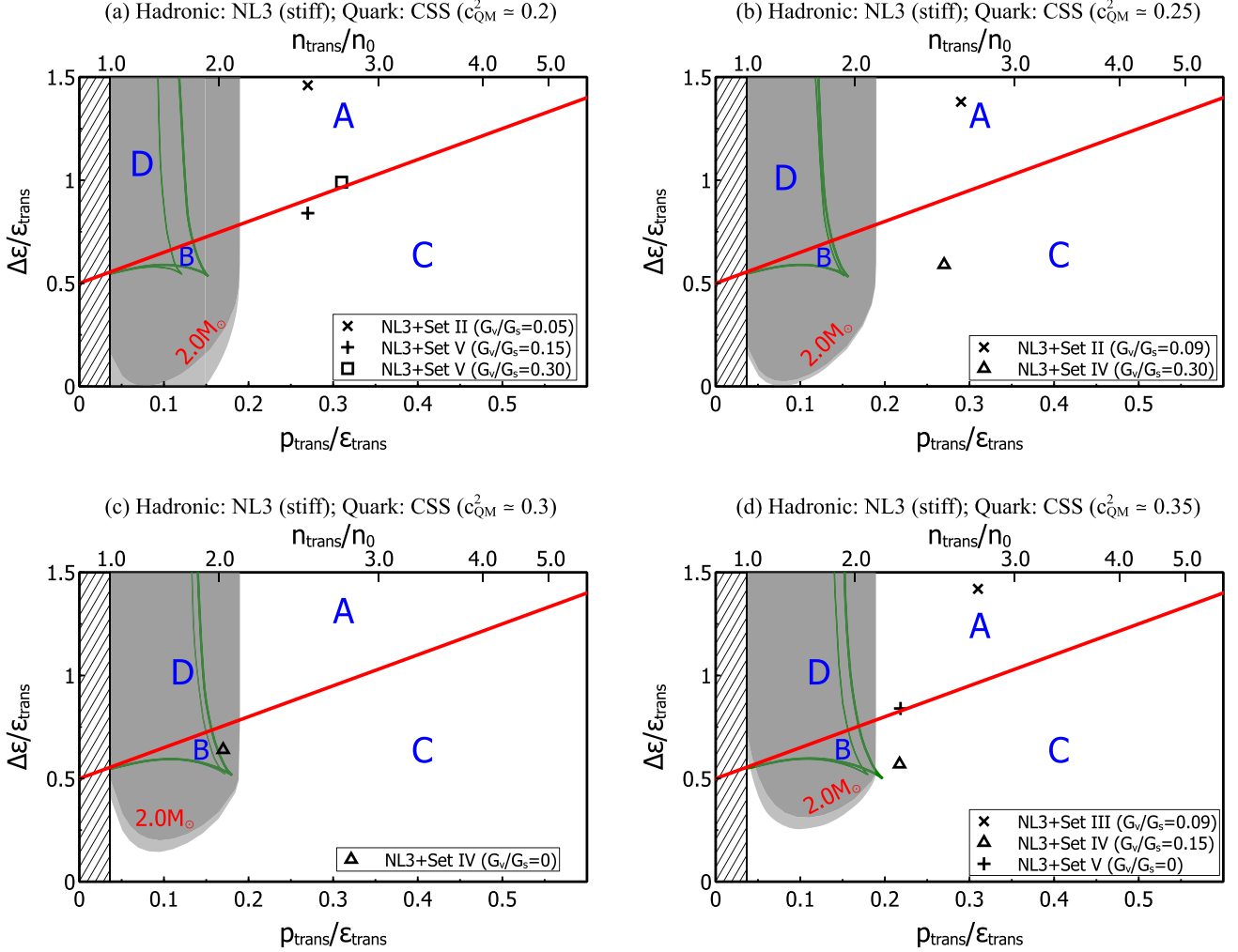


FIG. 6. Diagram showing (black symbols) where different quark matter parametrizations, for the local and nonlocal models, combined with NL3 nuclear matter, fall in the CSS parameter space. Panels (a), (b), (c), and (d) are for $c_{\text{QM}}^2 \simeq 0.2$, $c_{\text{QM}}^2 \simeq 0.25$, $c_{\text{QM}}^2 \simeq 0.3$, and $c_{\text{QM}}^2 \simeq 0.35$, respectively. EoSs below the straight solid (red) line (regions B and C) yield a connected hybrid branch. EoSs within the shaded gray area are excluded because their heaviest star is below $2M_{\odot}$. The hatched area at densities $n_{\text{trans}} < n_0$ is excluded because uniform nuclear matter is not stable in that region. See Tables III and IV.

parametrization and that the CSS parametrization helps us to understand the characteristics of the hybrid stars predicted by the NJL model. As we see in Figs. 5 and 6 and in Fig. 4 of Ref. [24] quark-matter EoSs that are soft, with $c_{\text{QM}}^2 \lesssim 1/3$, are severely restricted by the $2M_{\odot}$ constraint. To meet it they must have a high transition pressure. When the transition pressure is high, approaching the pressure at which the hadronic star would become unstable anyway even without a transition to quark matter, the hybrid branch tends to be very short because, unless the transition to quark matter is very weakly first order, the appearance of the denser core of quark matter pushes the star close to the point of instability. This explains why in this work we only find very short connected hybrid branches and no disconnected hybrid branches. The NJL models studied here tend to have a low speed of sound. The $2M_{\odot}$ constraint then rules out disconnected branches (the B and D regions of Figs. 5 and 6) and requires a high transition pressure.

The fact that the hybrid branches are so short means that only a very small range of pressures above the transition to quark matter are physically attained in hybrid stars, so, because the CSS parametrization is essentially a Taylor expansion of $\varepsilon(p)$ around the transition, it is a very accurate representation of the quark-matter EoS over this range.

The CSS parametrization exposes the physical consequences of varying the parameters of the NJL quark-matter EoS. Tables III and IV show the mapping from the NJL parameters to the CSS parameters. We see the following.

- (i) Increasing m_s at fixed vector to scalar coupling ratio, which corresponds to going from Set I to III (nonlocal NJL) or IV to V (local NJL), leads to an EoS with higher phase transition pressure, a larger energy density discontinuity at the transition, and higher speed of sound in the quark matter.

- (ii) Increasing the vector to scalar coupling ratio with other parameters held fixed also increases the transition pressure, energy density discontinuity, and speed of sound.
- (iii) The consequences for hybrid stars can be read off from Figs. 5 and 6. Increasing the strange quark mass or the repulsive vector interaction does not favor hybrid stars because at higher transition pressure and energy density discontinuity it becomes more likely that a quark-matter core will destabilize the star.

In the future, it would be useful to study further variations on the models considered here. This will help to shed light on how generic our results are. For hadronic matter, it would be interesting to use the DD2-EV EoS [15], which is a relativistic model that has been calibrated to fit known properties of nuclear matter. For quark matter, one should study the role of the mixing (\prime tHooft) term. It is known that the \prime tHooft interaction shifts the critical end-point location in the QCD

phase diagram, affecting the nature of the hadron-quark phase transition (see, for example, Refs. [77] and [79]). In addition, one could include a diquark coupling. The presence of diquark condensates lowers the transition chemical potential, allowing a lower transition pressure, which has been seen to yield longer hybrid branches than we found in this work [12].

ACKNOWLEDGMENTS

F.W. is supported by the U.S. National Science Foundation under Grant No. PHY-1411708. I.F.R.-S., G.A.C., and M.G.O. acknowledge financial support by UNLP (Argentina), Projects No. 11/G119 and No. 11/X718 (G.A.C.) and by CONICET (Argentina). M.G.A. and S.H. are supported by the U.S. Department of Energy, Office of Science, Office of Nuclear Physics under Award No. DE-FG02-05ER41375, and by the DOE Topical Collaboration Neutrinos and Nucleosynthesis in Hot and Dense Matter Contract No. DE-SC0004955.

-
- [1] P. Demorest, T. Pennucci, S. Ransom, M. Roberts, and J. Hessels, Shapiro delay measurement of a two solar mass neutron star, *Nature (London)* **467**, 1081 (2010).
 - [2] J. Antoniadis *et al.*, A massive pulsar in a compact relativistic binary, *Science* **340**, 6131 (2013).
 - [3] L. Bonanno and A. Sedrakian, Composition and stability of hybrid stars with hyperons and quark color-superconductivity, *Astron. Astrophys.* **539**, A16 (2012).
 - [4] M. Orsaria, H. Rodrigues, F. Weber, and G. A. Contrera, Quark deconfinement in high-mass neutron stars, *Phys. Rev. C* **89**, 015806 (2014).
 - [5] B. Bhowmick, M. Bhattacharya, A. Bhattacharyya, and G. Gangopadhyay, Massive neutron stars with a hyperonic core: A case study with the IUFSU relativistic effective interaction, *Phys. Rev. C* **89**, 065806 (2014).
 - [6] F. Weber, G. A. Contrera, M. G. Orsaria, W. Spinella, and O. Zubairi, Properties of high-density matter in neutron stars, *Mod. Phys. Lett. A* **29**, 1430022 (2014).
 - [7] T. Kojo, P. D. Powell, Y. Song, and G. Baym, Phenomenological QCD equation of state for massive neutron stars, *Phys. Rev. D* **91**, 045003 (2015).
 - [8] Z. Fodor and S. D. Katz, Finite T/μ lattice QCD and the critical point, *Prog. Theor. Phys. Suppl.* **153**, 86 (2004).
 - [9] A. Barducci, R. Casalbuoni, G. Pettini, and L. Ravagli, Calculation of the QCD phase diagram at finite temperature, and baryon and isospin chemical potentials, *Phys. Rev. D* **69**, 096004 (2004).
 - [10] J. L. Zdunik, P. Haensel, and R. Schaeffer, Phase transitions in stellar cores. II. Equilibrium configurations in general relativity, *Astron. Astrophys.* **172**, 95 (1987).
 - [11] M. G. Alford, S. Han, and M. Prakash, Generic conditions for stable hybrid stars, *Phys. Rev. D* **88**, 083013 (2013).
 - [12] T. Klahn, D. Blaschke, F. Sandin, C. Fuchs, A. Faessler, H. Grigorian *et al.*, Modern compact star observations and the quark matter equation of state, *Phys. Lett. B* **654**, 170 (2007).
 - [13] T. Klahn, R. Lastowiecki, and D. B. Blaschke, Implications of the measurement of pulsars with two solar masses for quark matter in compact stars and heavy-ion collisions: A Nambu-Jona-Lasinio model case study, *Phys. Rev. D* **88**, 085001 (2013).
 - [14] S. Benic, Heavy hybrid stars from multi-quark interactions, *Eur. Phys. J. A* **50**, 111 (2014).
 - [15] S. Benic, D. Blaschke, D. E. Alvarez-Castillo, T. Fischer, and S. Typel, A new quark-hadron hybrid equation of state for astrophysics. I. High-mass twin compact stars, *Astron. Astrophys.* **577**, A40 (2015).
 - [16] D. B. Blaschke, D. Gomez Dumm, A. G. Grunfeld, T. Klahn, and N. N. Scoccola, Hybrid stars within a covariant, nonlocal chiral quark model, *Phys. Rev. C* **75**, 065804 (2007).
 - [17] S. Benic, D. Blaschke, G. A. Contrera, and D. Horvatic, Medium induced Lorentz symmetry breaking effects in non-local Polyakov–Nambu–Jona-Lasinio models, *Phys. Rev. D* **89**, 016007 (2014).
 - [18] N. Yasutake, R. Lastowiecki, S. Benic, D. Blaschke, T. Maruyama, and T. Tatsumi, Finite-size effects at the hadron-quark transition and heavy hybrid stars, *Phys. Rev. C* **89**, 065803 (2014).
 - [19] A. Kurkela, P. Romatschke, and A. Vuorinen, Cold quark matter, *Phys. Rev. D* **81**, 105021 (2010).
 - [20] K. Schertler, C. Greiner, J. Schaffner-Bielich, and M. H. Thoma, Quark phases in neutron stars and a ‘third family’ of compact stars as a signature for phase transitions, *Nucl. Phys. A* **677**, 463 (2000).
 - [21] S. Banik and D. Bandyopadhyay, Color superconducting quark matter core in the third family of compact stars, *Phys. Rev. D* **67**, 123003 (2003).
 - [22] M. Alford, M. Braby, M. Paris, and S. Reddy, Hybrid stars that masquerade as neutron stars, *Astrophys. J.* **629**, 969 (2005).
 - [23] T. Klahn and T. Fischer, Vector interaction enhanced bag model for astrophysical applications, *Astrophys. J.* **810**, 134 (2015).
 - [24] M. G. Alford, G. F. Burgio, S. Han, G. Taranto, and D. Zappala, Constraining and applying a generic high-density equation of state, *Phys. Rev. D* **92**, 083002 (2015).
 - [25] T. Klahn, C. D. Roberts, L. Chang, H. Chen, and Y.-X. Liu, Cold quarks in medium: An equation of state, *Phys. Rev. C* **82**, 035801 (2010).
 - [26] U. Vogl and W. Weise, The Nambu and Jona Lasinio model: Its implications for hadrons and nuclei, *Prog. Part. Nucl. Phys.* **27**, 195 (1991).

- [27] S. P. Klevansky, The Nambu-Jona-Lasinio model of quantum chromodynamics, *Rev. Mod. Phys.* **64**, 649 (1992).
- [28] T. Hatsuda and T. Kunihiro, QCD phenomenology based on a chiral effective Lagrangian, *Phys. Rep.* **247**, 221 (1994).
- [29] M. Buballa, NJL model analysis of quark matter at large density, *Phys. Rep.* **407**, 205 (2005).
- [30] J. Praschifka, R. T. Cahill, and C. D. Roberts, Mesons and diquarks in chiral QCD: Generation of constituent quark masses, *Int. J. Mod. Phys. A* **4**, 4929 (1989).
- [31] R. D. Ball, Mesons, skyrmions and baryons, *Int. J. Mod. Phys. A* **5**, 4391 (1990).
- [32] S. M. Schmidt, D. Blaschke, and Yu. L. Kalinovsky, Scalar-pseudoscalar meson masses in nonlocal effective QCD at finite temperature, *Phys. Rev. C* **50**, 435 (1994).
- [33] R. S. Plant and M. C. Birse, Meson properties in an extended nonlocal NJL model, *Nucl. Phys. A* **628**, 607 (1998).
- [34] G. Ripka, *Quarks Bound by Chiral Fields: The Quark-Structure of the Vacuum and of Light Mesons and Baryons* (Oxford University Press, Oxford, U.K., 1997).
- [35] D. Gomez Dumm, A. G. Grunfeld, and N. N. Scoccola, On covariant nonlocal chiral quark models with separable interactions, *Phys. Rev. D* **74**, 054026 (2006).
- [36] G. A. Contrera, D. Gomez Dumm, and N. N. Scoccola, Nonlocal SU(3) chiral quark models at finite temperature: The role of the Polyakov loop, *Phys. Lett. B* **661**, 113 (2008).
- [37] D. Diakonov and V. Yu. Petrov, A theory of light quarks in the instanton vacuum, *Nucl. Phys. B* **272**, 457 (1986).
- [38] T. Schaefer and E. V. Shuryak, Instantons in QCD, *Rev. Mod. Phys.* **70**, 323 (1998).
- [39] C. D. Roberts and A. G. Williams, Dyson-Schwinger equations and their application to hadronic physics, *Prog. Part. Nucl. Phys.* **33**, 477 (1994).
- [40] C. D. Roberts and S. M. Schmidt, Dyson-Schwinger equations: Density, temperature and continuum strong QCD, *Prog. Part. Nucl. Phys.* **45**, S1 (2000).
- [41] M. B. Parappilly, P. O. Bowman, U. M. Heller, D. B. Leinweber, A. G. Williams, and J. B. Zhang, Scaling behavior of quark propagator in full QCD, *Phys. Rev. D* **73**, 054504 (2006).
- [42] R. D. Bowler and M. C. Birse, A Nonlocal, covariant generalization of the NJL model, *Nucl. Phys. A* **582**, 655 (1995).
- [43] W. Broniowski, B. Goll, and G. Ripka, Solitons in nonlocal chiral quark models, *Nucl. Phys. A* **703**, 667 (2002).
- [44] A. H. Rezaeian, N. R. Walet, and M. C. Birse, Baryon structure in a quark-confining non-local NJL model, *Phys. Rev. C* **70**, 065203 (2004).
- [45] G. A. Contrera, D. G. Dumm, and N. N. Scoccola, Meson properties at finite temperature in a three flavor nonlocal chiral quark model with Polyakov loop, *Phys. Rev. D* **81**, 054005 (2010).
- [46] M. G. Alford, A. Schmitt, K. Rajagopal, and T. Schafer, Color superconductivity in dense quark matter, *Rev. Mod. Phys.* **80**, 1455 (2008).
- [47] J. Schaffner-Bielich, M. Hanauske, H. Stoecker, and W. Greiner, Phase Transition to Hyperon Matter in Neutron Stars, *Phys. Rev. Lett.* **89**, 171101 (2002).
- [48] B. K. Agrawal, Equations of state and stability of color-superconducting quark matter cores in hybrid stars, *Phys. Rev. D* **81**, 023009 (2010).
- [49] J. D. Walecka, A theory of highly condensed matter, *Ann. Phys.* **83**, 491 (1974).
- [50] J. Boguta and A. Bodmer, Relativistic calculation of nuclear matter and the nuclear surface, *Nucl. Phys. A* **292**, 413 (1977).
- [51] J. Boguta and J. Rafelski, Thomas-Fermi model of finite nuclei, *Phys. Lett. B* **71**, 22 (1977).
- [52] J. Boguta and H. Stöcker, Systematics of nuclear matter properties in a non-linear relativistic field theory, *Phys. Lett. B* **120**, 289 (1983).
- [53] B. D. Serot and J. D. Walecka, The relativistic nuclear many body problem, *Adv. Nucl. Phys.* **16**, 1 (1986).
- [54] N. K. Glendenning and S. A. Moszkowski, Reconciliation of Neutron Star Masses and Binding of the Lambda in Hypernuclei, *Phys. Rev. Lett.* **67**, 2414 (1991).
- [55] G. A. Lalazissis, J. König, and P. Ring, A New parametrization for the Lagrangian density of relativistic mean field theory, *Phys. Rev. C* **55**, 540 (1997).
- [56] N. K. Glendenning, Neutron stars are giant hypernuclei? *Astrophys. J.* **293**, 470 (1985).
- [57] F. Weber, *Pulsars as Astrophysical Laboratories for Nuclear and Particle Physics* (IOP Publishing, Bristol, U.K., 1999).
- [58] K. Kashiwa, T. Hell, and W. Weise, Nonlocal Polyakov-Nambu-Jona-Lasinio model and imaginary chemical potential, *Phys. Rev. D* **84**, 056010 (2011).
- [59] G. A. Contrera, A. G. Grunfeld, and D. B. Blaschke, Phase diagrams in nonlocal Polyakov-Nambu-Jona-Lasinio models constrained by lattice QCD results, *Phys. Part. Nucl. Lett.* **11**, 342 (2014).
- [60] A. Scarpellini, D. Gomez Dumm, and N. N. Scoccola, Light pseudoscalar mesons in a nonlocal SU(3) chiral quark model, *Phys. Rev. D* **69**, 114018 (2004).
- [61] M. Orsaria, H. Rodrigues, F. Weber, and G. A. Contrera, Quark-hybrid matter in the cores of massive neutron stars, *Phys. Rev. D* **87**, 023001 (2013).
- [62] E. S. Fraga, R. D. Pisarski, and J. Schaffner-Bielich, New class of compact stars at high density, *Nucl. Phys. A* **702**, 217 (2002).
- [63] M. Buballa, F. Neumann, M. Oertel, and I. Shovkovy, Quark mass effects on the stability of hybrid stars, *Phys. Lett. B* **595**, 36 (2004).
- [64] R. Negreiros, V. A. Dexheimer, and S. Schramm, Quark core impact on hybrid star cooling, *Phys. Rev. C* **85**, 035805 (2012).
- [65] M. G. Alford, K. Rajagopal, S. Reddy, and F. Wilczek, Minimal CFL nuclear interface, *Phys. Rev. D* **64**, 074017 (2001).
- [66] K. Iida and K. Sato, Effects of hyperons on the dynamical deconfinement transition in cold neutron star matter, *Phys. Rev. C* **58**, 2538 (1998).
- [67] T. Endo, Region of hadron-quark mixed phase in hybrid stars, *Phys. Rev. C* **83**, 068801 (2011).
- [68] M. B. Pinto, V. Koch, and J. Randrup, The surface tension of quark matter in a geometrical approach, *Phys. Rev. C* **86**, 025203 (2012).
- [69] G. Lugones, A. G. Grunfeld, and M. Al Ajmi, Surface tension and curvature energy of quark matter in the Nambu-Jona-Lasinio model, *Phys. Rev. C* **88**, 045803 (2013).
- [70] W.-y. Ke and Y.-x. Liu, Interface tension and interface entropy in the 2+1 flavor Nambu-Jona-Lasinio model, *Phys. Rev. D* **89**, 074041 (2014).
- [71] L. F. Palhares and E. S. Fraga, Droplets in the cold and dense linear sigma model with quarks, *Phys. Rev. D* **82**, 125018 (2010).
- [72] J. Macher and J. Schaffner-Bielich, Phase transitions in compact stars, *Eur. J. Phys.* **26**, 341 (2005).

- [73] K. Masuda, T. Hatsuda, and T. Takatsuka, Hadron-quark crossover and massive hybrid stars with strangeness, *Astrophys. J. Lett.* **764**, 12 (2013).
- [74] Z. F. Seidov, The stability of a star with a phase change in general relativity theory, *Sov. Astron. Astron. Zh.* **15**, 347 (1971).
- [75] R. Schaeffer, L. Zdunik, and P. Haensel, Phase transitions in stellar cores. I. Equilibrium configurations, *Astron. Astrophys.* **126**, 121 (1983).
- [76] L. Lindblom, Phase transitions and the mass radius curves of relativistic stars, *Phys. Rev. D* **58**, 024008 (1998).
- [77] S. Klimt, M. F. M. Lutz, and W. Weise, Chiral phase transition in the SU(3) Nambu and Jona-Lasinio model, *Phys. Lett. B* **249**, 386 (1990).
- [78] G. Miniutti, J. A. Pons, E. Berti, L. Gualtieri, and V. Ferrari, Non-radial oscillation modes as a probe of density discontinuities in neutron stars, *Mon. Not. R. Astron. Soc.* **338**, 389 (2003).
- [79] K. Fukushima, Phase diagrams in the three-flavor Nambu-Jona-Lasinio model with the Polyakov loop, *Phys. Rev. D* **77**, 114028 (2008).